Molecular Dynamics on a Model for Nascent High-Density Lipoprotein: Role of Salt Bridges

Christopher Sheldahl and Stephen C. Harvey
Department of Biochemistry and Molecular Genetics, University of Alabama at Birmingham, Birmingham, Alabama 35294 USA

ABSTRACT The results of an all-atom molecular dynamics simulation on a discoidal complex made of 1-palmitoyl-2-oleoyl-*sn*-glycero-3-phosphocholine (POPC) and a synthetic α-helical 18-mer peptide with an apolipoprotein-like charge distribution are presented. The system consists of 12 acetyl-18A-amide (Ac-18A-NH_2) (Anantharamaiah et al., 1985. *J. Biol. Chem.* 260:10248–10255) molecules and 20 molecules of POPC in a bilayer, 10 in each leaflet, solvated in a sphere of water for a total of 28,522 atoms. The peptide molecules are oriented with their long axes normal to the bilayer (the "picket fence" orientation). This system is analogous to complexes formed in nascent high-density lipoprotein and to Ac-18A-NH_2/phospholipid complexes observed experimentally. The simulation extended over 700 ps, with the last 493 ps used for analysis. The symmetry of this system allows for averaging over different helices to improve sampling, while maintaining explicit all-atom representation of all peptides. The complex is stable on the simulated time scale. Several possible salt bridges between and within helices were studied. A few salt bridge formations and disruptions were observed. Salt bridges provide specificity in interhelical interactions.

INTRODUCTION

Discoidal lipoprotein complexes

Lipoproteins are noncovalently associated lipid/protein complexes that are involved in lipid transport. One of the most significant classes is high-density lipoprotein (HDL). The concentration of HDL in the blood is inversely correlated with atherosclerosis and is involved in cholesterol transport and metabolism, including the activation of lecithin:cholesterol acyltransferase (LCAT) (Segrest et al., 1994). The major protein component of HDL is Apo A-I (Segrest et al., 1994; Brouillette and Anantharamaiah, 1995). The principal structural motif involved in Apo A-I/lipid interaction is the amphipathic α-helix (Segrest et al., 1994; Brouillette and Anantharamaiah, 1995; Borhani et al., 1997).

When Apo A-I is mixed with certain phospholipids, there is spontaneous formation of small ($<$200 Å in diameter) lipid/protein complexes. These are discoidal in shape, as observed by electron microscopy (Tall et al., 1977) and x-ray scattering (Atkinson et al., 1976). These discs are similar in shape and size to nascent HDL. The discs are believed to be patches of lipid bilayer with protein surrounding the nonpolar acyl chains of the lipids (Segrest, 1977; Atkinson et al., 1980). Synthetic amphipathic helix peptides have been experimentally found to form similar complexes with lipid (Anantharamaiah et al., 1985).

The orientation of the amphipathic helices at the edge of these discoidal complexes is a subject of some interest. Several infrared spectroscopy studies using various peptides and proteins indicate that the amphipathic helices in these discs are oriented with their long axes perpendicular to the plane of the bilayer (Brasseur et al., 1990; Wald et al., 1990; Corijn et al., 1993). This orientation (the "picket fence" model) is similar to the orientations found in transmembrane helices. However, the recent crystal structure of an N-terminal deletion mutant of Apo A-I in solution provides very suggestive evidence that in Apo A-I/lipid complexes the helices are perpendicular to the lipid chains (the "rail fence" model) (Borhani et al., 1997). Furthermore, in the complex formed between *Manduca sexta* apolipophorin III and 1-myristyl-2-myristyl-*sn*-3-phosphocholine (DMPC), the helices of the protein appear to have their long axes in the rail fence orientation as well (Raussens et al., 1995). Orientations intermediate between the picket fence and rail fence orientations may exist.

The helices found in apolipoproteins that are most highly correlated with lipid affinity have a characteristic charge distribution (Segrest et al., 1994). This type of amphipathic helix, called class A, has positively charged residues forming the boundary between the polar and nonpolar faces of the helix and negatively charged residues in the center of the polar face. The role of this charge distribution has been studied with the synthetic 18-mer class A amphipathic helix 18A and peptides with related sequences. Fig. 1 gives the sequence of 18A, as well as a schematic view down the helix axis of 18A in an α-helix conformation. Note that this peptide has the class A charge distribution. This peptide forms discoidal complexes with DMPC (Anantharamaiah et al., 1985). Discoidal complexes composed of Ac-18A-NH_2 and phospholipid are potent activators of LCAT (Chung et

Received for publication 18 May 1998 and in final form 17 November 1998.

Address reprint requests to Dr. Stephen C. Harvey, Department of Biochemistry and Molecular Genetics, University of Alabama at Birmingham, Birmingham, AL 35294. Tel.: 205-934-5028; Fax: 205-975-2547; E-mail: harvey@neptune.cmc.uab.edu.

0006-3495/99/03/1190/09 $2.00

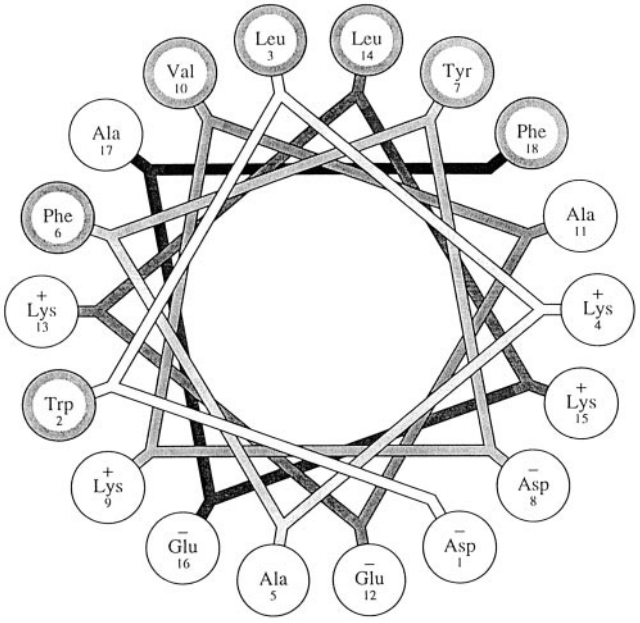

FIGURE 1 Sequence and helical wheel diagram for the 18A peptide. This figure was generated with WHEEL (Jones et al., 1992).

al., 1985). A related peptide, 18R, in which the relative positions of the positively charged and negatively charged residues have been reversed, has also been studied. The 18R peptide forms less stable complexes with phospholipid (Anantharamaiah et al., 1985). The charge distribution is not believed to be involved in headgroup-peptide interactions, because no difference in headgroup behavior has been observed in peptide/lipid complexes with 18A-like peptides or with 18R-like peptides (Epand et al., 1989). This observation also suggests that the picket fence orientation may be preferred for this series of peptides.

Salt bridges and the stabilization of protein structure

Both intrahelix and interhelix salt bridges have been seen in the crystal structures of apolipoproteins in an aqueous environment (Borhani et al., 1997; Wilson et al., 1991). However, the extent to which these may be artifacts of crystallization is not known. The possibility of solvent-exposed salt bridges in proteins has been investigated both experimentally and theoretically (Nakamura, 1996). According to continuum electrostatic calculations (Hendsch and Tidor, 1994), solvent-exposed salt bridges are generally destabilizing relative to isosteric hydrophobic interactions, because of a greater attraction of the residues for water than for each other. Experimental results consistent with a minimal role for solvent-exposed salt bridges are given in a variety of studies. Among these was a study (Bradley et al., 1990) that failed to detect intrahelical salt bridging in synthetic peptides. Salt bridging was also not found between the helices of the GCN4 leucine zipper in solution (Lumb and Kim, 1995), although it is seen in the crystal structure. However, other studies have found some role for salt bridging in solution (Marqusee and Baldwin, 1987; Huyghues-Despointes and Baldwin, 1997; Lyu et al., 1992; Smith and Scholtz, 1998). Most of these have found a favorable free energy for solvent-exposed salt bridges of ~0.5 kcal/mol. A free energy of 3–5 kcal/mol has been observed for a partially solvent-accessible salt bridge in T4 lysozyme (Anderson et al., 1990). It is clear that salt bridging can be significant, at least as a determinant of specificity in some systems, possibly including lipoproteins.

Salt bridges in 18A series peptides

Because apolipoproteins may be expected to show specific interactions between different helices, as has been observed in relevant protein crystal structures (Borhani et al., 1997; Breiter et al., 1991; Wilson et al., 1991), the forces responsible for creating specificity in interhelix interactions are of interest. One possibility, considering the conserved class A charge distribution, is that this charge distribution is important in interhelix salt bridges or other interactions, such as interactions between charged residues and polar ones.

The possibility of salt bridging in 18A and the related 18R peptides has been addressed experimentally (Lund-Katz et al., 1995). By examining the pK_a values of dimethyl-Lys analogs of these peptides when bound to DMPC discs, they judged whether a particular Lys residue formed a salt bridge. They saw pK_a shifts consistent with salt bridge formation (or another favorable interaction) in Lys^{15} and Lys^{4}, but not Lys^{13} or Lys^{9}. It is unclear what the salt bridge partners of these residues are. It is also not known what effect the dimethylation may have had on salt bridge formation.

Molecular dynamics simulations of membranes

Many molecular dynamics simulations of membrane systems have now appeared. The systems studied include lipid bilayers (Chiu et al., 1995; Damodaran et al., 1992; Huang et al., 1994; Damodaran and Merz, 1994; Pastor, 1994; Heller et al., 1993; Tu et al., 1995; Zhou and Schulten, 1995), bilayer-peptide (or bilayer-protein) systems (Damodaran and Merz, 1995; Damodaran et al., 1995; Edholm et al., 1995; Woolf and Roux, 1996; Huang and Loew, 1995; Phillips et al., 1997), and bilayer–small molecule systems (Alper and Stouch, 1995; Bassolino-Klimas et al., 1995; Edholm and Nyberg, 1992). Impressive demonstration of agreement with various experimental properties has been demonstrated in these simulations. The simulations have typically treated 10,000–30,000 atoms and have extended to the several hundred picosecond range. This may not be long enough to sample all behaviors of interest. An alternative approach to membrane simulations is to treat only small sections of the membrane, such as a few lipids, explicitly and account for solvent and other lipids by using a mean field potential (De Loof et al., 1991; Pearce and Harvey,

1993). The latter approach has advantages with respect to time equilibration, but is at a disadvantage with respect to equilibration in space. Neither method reaches the combination of sufficiently large system size and sufficiently long time scale necessary for examining collective motions.

In this work we present the results of a molecular dynamics simulation on a picket fence model for the 18A/POPC discoidal complex. Interhelical interactions in this complex are studied. This simulation on a picket fence model for the 18A/POPC complex is the first in a planned series of simulations that will investigate these aspects of lipoprotein structure and dynamics in detail.

METHODS

Construction of the system

Using the molecular modeling program Sybyl (Tripos Associates, St Louis, MO), two Ac-18A-NH2 peptides in α-helix configurations were placed with their centers 10 Å apart. They were oriented in an antiparallel fashion. The antiparallel orientation was chosen to create favorable helix-dipole interactions and to maximize relevance to natural lipoproteins, because this orientation is found in apolipoprotein crystal structures (Borhani et al., 1997; Breiter et al., 1991; Wilson et al., 1991). The side-chain orientations of Lys, Trp, and Tyr residues were then altered to place their hydrophilic groups toward the hydrophilic side of the dimer and hydrophobic groups toward the other face. This "snorkeled" conformation has been postulated based on experimental evidence (Mishra et al., 1994). No other modifications to the ideal helix structure were made at this point. The resulting dimer was then copied and rotated to form a circle of 12 helices with an outer diameter of ~60 Å.

At this point, a patch of 10 POPC molecules from one leaflet of the central portion of the simulation of fluid-phase POPC by Heller et al. (1993) was used as the starting structure for the lipid bilayer. These lipids were then copied to form a bilayer of 20 lipids (10 lipids in each monolayer). The resulting patch of lipid formed the lipid portion of the simulated system. The peptide portion and the lipid portion of the system were then combined.

Using the program X-PLOR (Brünger, 1992), hydrogens were added, and then the peptide/lipid complex was minimized in vacuo by the application of 10,000 steps of a conjugate gradient minimization algorithm. The CHARMM force field (version 22) (Brooks et al., 1983; MacKerell et al., 1998; Schlenkrich et al., 1996) was used for this and all subsequent simulations. Parameters for the POPC double bond were adapted from parameters recently developed to work with the CHARMM force field (Feller et al., 1997). The TIP3P water model was used (Jorgensen et al., 1983). A distance-dependent dielectric constant ($D = R$ in Å) was used as a crude model for electrostatic screening by water molecules during this minimization.

The minimized complex was then solvated in an 84-Å-diameter sphere of water. Water molecules that were within 2.5 Å of any complex atom or that were within the approximate confines of the lipid acyl chain region were deleted. The entire system was then energy minimized (conjugate gradient), using X-PLOR for 7500 steps. The dielectric constant was set to 1, regardless of distance, for this minimization and for all subsequent modeling. An electrostatic cutoff of 10 Å was used.

Molecular dynamics: simulation and analysis

Using the program NAMD (Nelson et al., 1996), the minimized, solvated system was heated from 10 K to 300 K over a period of 30 ps via molecular dynamics. Velocities were assigned every picosecond and raised in 10 K intervals. Velocity rescaling was used to maintain a constant temperature during each picosecond. Spherical boundary conditions, as implemented in NAMD, were used to prevent waters from leaving the system, with a boundary of 45 Å and a force constant of 30 kcal/Å^2. At this point the system was simulated using NAMD for a total of 703 ps at 300 K with velocity rescaling. Over the last 493 ps, coordinates were saved every picosecond and used for the analysis. The programs VMD (Humphrey et al., 1996) and Ribbons (Carson, 1991) were used to visualize the system. Scripts written in the X-PLOR language (Brünger, 1992) and our own programs were used for analysis.

RESULTS AND DISCUSSION

Overall structure of the system

Fig. 2 shows a space-filling view of the lipid and peptide portions of the system at the end of the simulation. The view is perpendicular to the long axes of the helices (a "side" view). Fig. 3 is a view parallel to the long axes of the peptide helices (a "top" view). Taken together, these figures indicate that the helices are closely packed. This packing was stable on the simulated time scale.

Fig. 4 shows the scheme used to divide the POPC molecule into groups for Fig. 5, which is a plot of the probability of finding each type of atom at various distances perpendicular to the membrane. Water oxygen atoms are included in Fig. 5 only if they are less than 10 Å from the radial center of the disk, so as to ignore those waters at the sides of the complex. Fig. 5 shows that the lipid atoms are distributed along the bilayer normal in a manner similar to that seen in simulation (Heller et al., 1993) and in experiment (Wiener and White, 1992) for pure lipid bilayers. The interleaflet minimum in lipid density is not duplicated very well, however, even though the phosphate-to-phosphate distance across the bilayer is very similar that to these previous studies. It can be seen that the peptide atoms extend along the hydrocarbon chains of the lipids, indicating that Ac-18A-NH_2 and POPC have similar lengths. This suggests that the picket fence model is plausible for this peptide's discoidal complexes with lipid. During the simulation, water penetrated the bilayer up to the acyl (carbonyl) atoms, as observed in experimental studies of pure bilayers (Wiener and White, 1992).

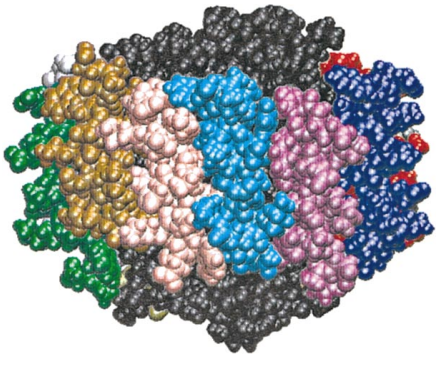

FIGURE 2 View of the Ac-18A-NH_2/POPC complex perpendicular to the long axes of the helices. The lipid is shown in black. The different peptide helices are shown in various colors. This was generated with VMD (Humphrey et al., 1996).

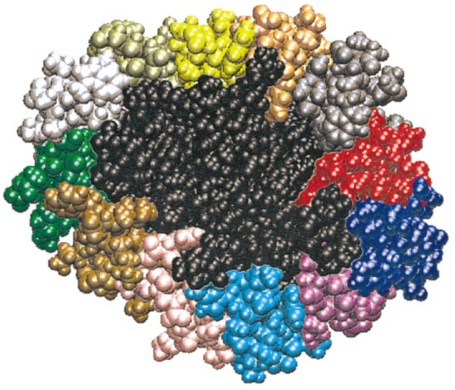

FIGURE 3 View of the Ac-18A-NH_2/POPC complex parallel to the long axes of the helices. The lipid is shown in black. The different peptide helices are shown in various colors. This was generated with VMD (Humphrey et al., 1996).

Fig. 6 displays a histogram of atom number density along the radial dimension to examine the extent of peptide interaction with the lipid bilayer. Water oxygens are included if they have a Z coordinate between -10 and 10 Å, thus ignoring the waters along the top and bottom of the disk. In Fig. 6, the lipid density extends to the center of the peptide peak. There is minimal overlap of the lipid and water peaks. It is also evident that there is some water between helices, because the water peak extends well into the peptide peak.

Interpeptide salt bridges

Fig. 7 displays four peptide monomers taken from the simulation and illustrates that two distinct interfaces exist. In one the Asp^8 and Lys^{15} residues from two neighboring helices are present. These residues are not present in the other interface. The former will be designated as the "odd" interface, the latter as the "even."

Because the interactions between helices are of interest, histograms of the interpeptide energy were made. These were averaged over all "odd" or "even" interfaces and over all 493 ps. Solvent-peptide interactions were ignored in these calculations, and a constant dielectric constant of 1 was used, because this was simply a ranking procedure. These histograms reveal a difference in the energetics of the two types of interface. The peptide-peptide mean interaction energy is about -100 (nominal) kcal/mol for the odd interface, whereas it is roughly zero for the even interface (Figs.

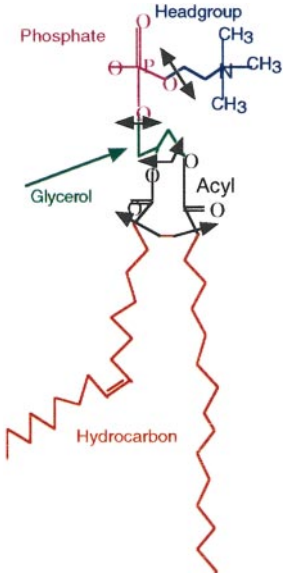

FIGURE 4 The scheme used to divide lipid atoms for Fig. 5.

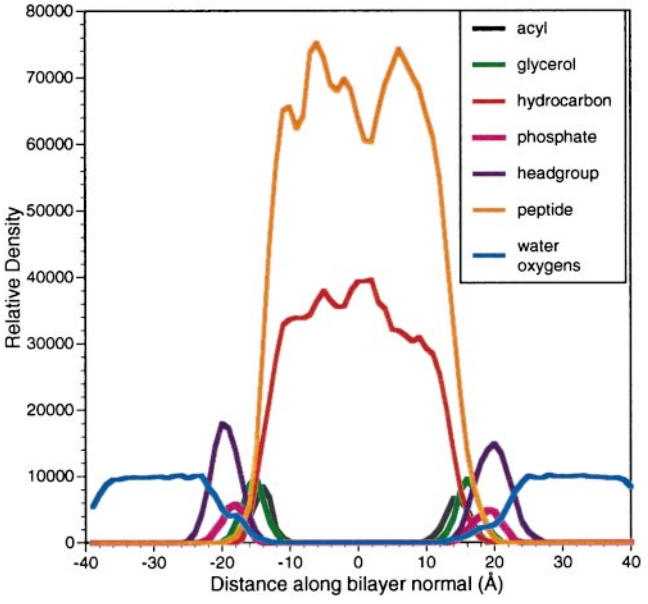

FIGURE 5 Probability distribution functions of atomic positions along the bilayer normal i.e., parallel to the long axes of the helices, averaged over all time frames.

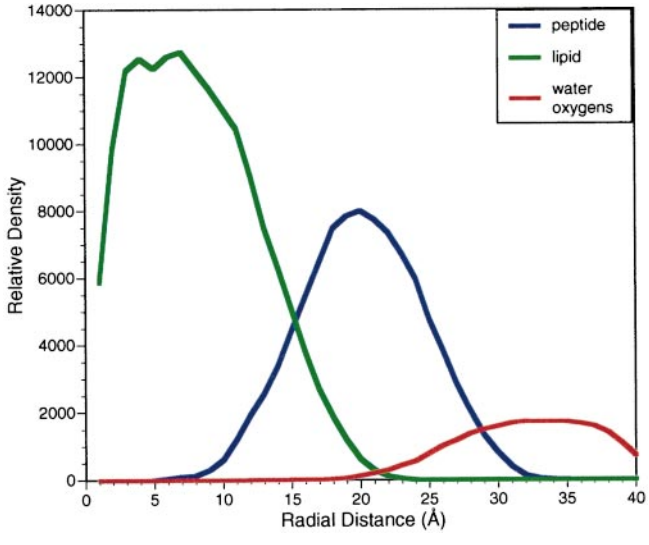

FIGURE 6 Probability distribution function along the radial dimension, averaged over all time frames.

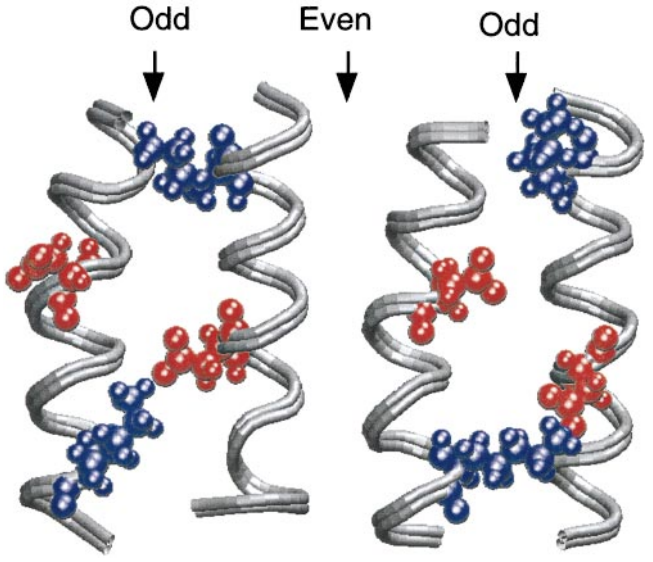

FIGURE 7 Illustration of the two types of interpeptide interfaces. Asp_8 (*red*) and Lys_{15} (*blue*) are shown in a space-filling representation. This was generated with Ribbons (Carson, 1991).

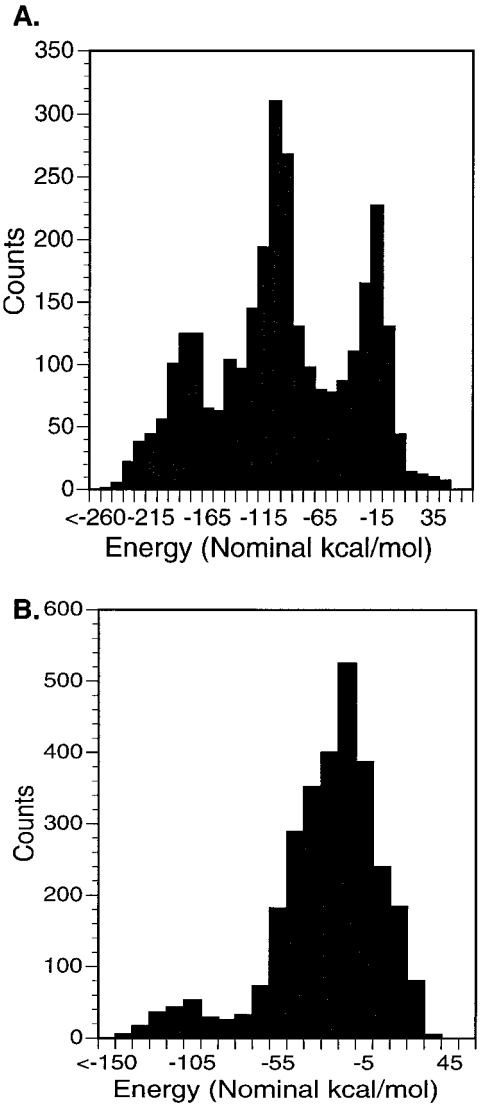

FIGURE 8 Probability distribution function of interpeptide interaction energy for the odd (*A*) and even (*B*) interfaces, averaged over all helices and all time frames.

8 and 9). Furthermore, the distribution of energies for the odd interface has three maxima, whereas there are only two distinct maxima in the even interface energy distribution.

To understand the maxima in the interpeptide energy probability energy, the number of interhelix salt bridges (defined as acidic carboxylate carbon and basic amino nitrogen side-chain atoms within 4.8 Å) versus interpeptide energy was plotted (Fig. 9). For the odd interface (Fig. 9 *A*) there are zero, one, or two salt bridges, corresponding to the three maxima seen in the energy histogram. Similarly for the even interface (Fig. 9 *B*), there are zero or one salt bridges observed, corresponding to the appropriate energy histogram maxima. This could have been postulated based on the energy histograms alone, because the energy difference between maxima is ~100 kcal/mol, which is the energy of a pair of electron charges when separated by ~3 Å in a vacuum. Salt bridging alone is able to explain the principal features of the energy distributions.

The principal interaction in the odd interfaces was found to be an Asp^8-Lys^{15} salt bridge. The even interface interaction energies were dominated by a Glu^{12}-Lys^9 salt bridge. As a means of studying the time- and monomer-averaged behavior of these salt bridges, relative radial distribution functions (RDFs) were calculated for each of these salt bridges. The value of the RDF (ρ) for a given value of the distance between two atoms of interest is given by

$$\rho(R) = (N/R^2) \quad (1)$$

where N is the total number of cases (for all copies of the salt bridge and all time steps) in which the distance between the atoms is in a narrow bin (0.1 Å wide), with an upper limit R. The atoms selected for these RDFs were the carboxylate carbons of Asp and Glu and the side-chain nitrogen of Lys. RDFs for the principal interhelix salt bridges are given in Fig. 10. The peak centered at ~2.5–4.8 Å in each RDF represents the salt-bridged structures. The second peak, with a maximum at ~6 Å for the odd interface (Fig. 10 *A*) and at 8 Å for the even interface (Fig. 10 *B*) represents the most favorable non-salt-bridged distance. Note that the Asp^8-Lys^{15} salt bridge appears to be stronger than the Glu^{12}-Lys^9 interaction.

Intrapeptide salt bridges

The possibility of salt-bridging within helices was also investigated. Intrapeptide salt bridges are another possible explanation for the experimental pK_a results (Lund-Katz et al., 1995). In addition, intrapeptide salt bridges provide more opportunities to study the general phenomenon of salt

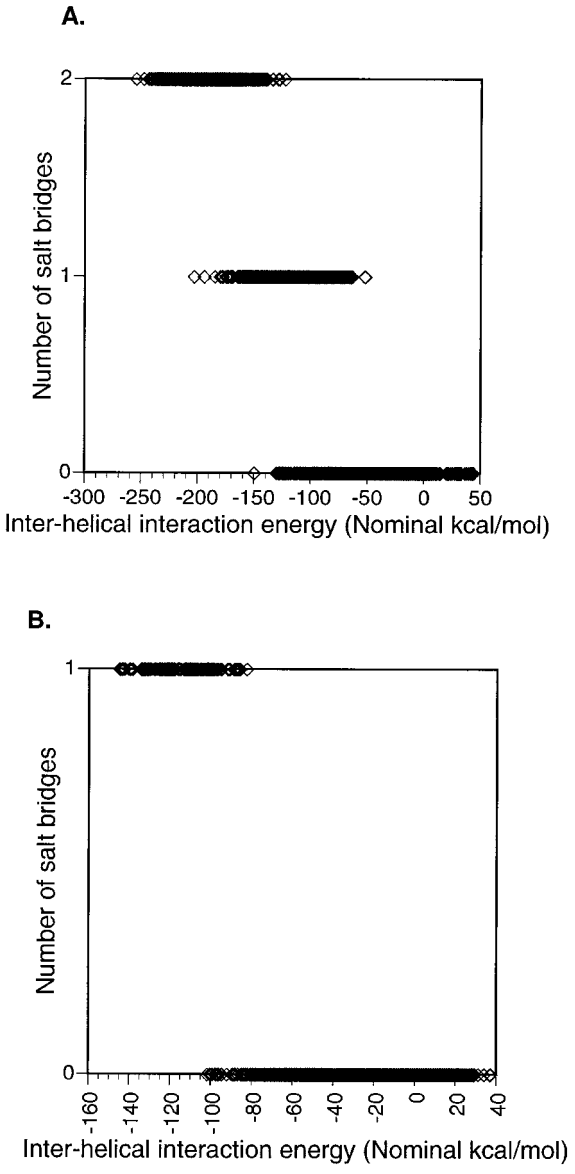

FIGURE 9 Number of interhelix salt bridges versus interpeptide interaction energy for the odd (*A*) and even (*B*) interfaces, averaged over all helices and all time frames.

bridging in peptides and proteins. Because there are 3.6 residues per turn in an ideal α-helix, possible (i, $i + 3$) and (i, $i + 4$) intrahelical salt bridges were studied. There are four possible (i, $i + 3$) salt bridges in 18A (D1-K4, K9-E12, E12-K15, K13-K16) and one possible (i, $i + 4$) salt bridge (K4-D8). Time- and helix-averaged RDFs (Fig. 11) were calculated for all possible (i, $i + 3$) and (i, $i + 4$) intrahelical salt bridges. The carboxylate carbon of acidic residues and the NZ atom of basic residues (lysines) were chosen for these graphs. The three salt bridges with Lys as the N-terminal member of the pair (K4-D8, K9-E12, K13-E16) did show significant formation. One of the remaining possible salt bridges showed very weak formation (D1-K4), whereas the other showed none (E12-K15).

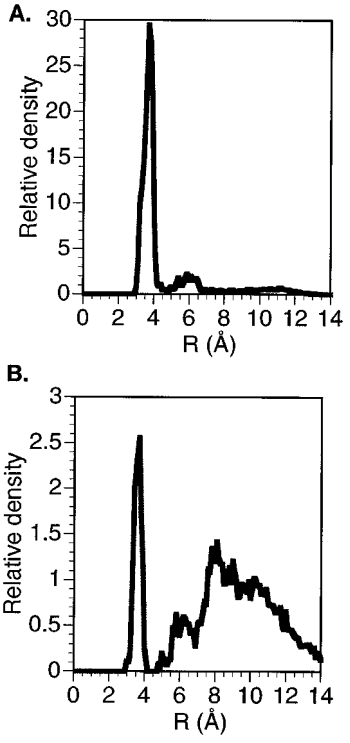

FIGURE 10 Lysine nitrogen-acidic side-chain carboxylate carbon RDF for the odd interface D8-K15 salt bridge (*A*) and the even interface K9-E12 salt bridge (*B*) (all helices and all time frames).

Salt bridge dynamics

Characterization of the time scales of salt bridge formation and disruption is essential in evaluating the ability of molecular dynamics to investigate the process.

The number of transitions between the salt-bridged and non-salt-bridged states was calculated for the significant salt bridges (two interhelix, three intrahelix salt bridges). A distance criterion based on the RDFs was used. The transitions were counted using the "simple counting" procedure (Loncharich et al., 1992). The total numbers of salt bridge formations and salt bridge disruptions are shown for the significant salt bridges in Table 1. The results are shown for all time steps and all helices. The salt-bridging residue pair that interconverts between states the most quickly (the interhelix odd interface interhelix interaction D8-K15) shows five formations and five disruptions during the simulation. Because there are 12 copies of this salt bridge, there is an average of ~0.4 formations and ~0.4 disruptions per salt bridge copy for this pair. This would mean one formation and one disruption for each particular copy of this salt bridge in ~1.2 ns. The slowest interconverting salt bridges (intrahelix K4-K8 and even interface interhelix K9-E12) each show only one formation and no disruptions. This gives an average of ~6.9 ns for the salt-bridge formation for a particular copy of this salt bridge. In all, 11 formations and 13 disruptions were observed for all of the salt bridges listed in Table 2. Thus the mean lifetime for salt bridges is estimated to be in the range of 1–10 ns.

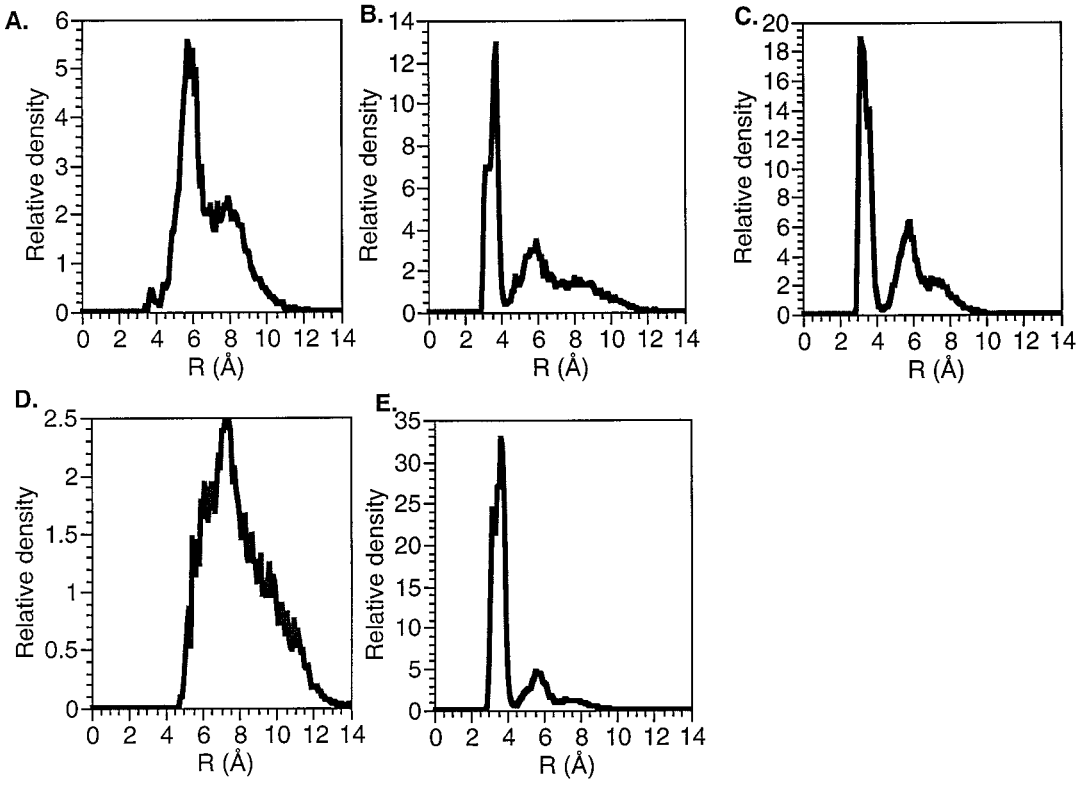

FIGURE 11 Lysine nitrogen-acidic side-chain carboxylate carbon RDF for the possible (i, $i + 3$) and (i, $i + 4$) intrahelical salt bridges, (*A*) D1-K4, (*B*) K4-D8, (*C*) K9-E12, (*D*) E12-K15, (*E*) K13-E16, averaged over all helices and all time frames.

CONCLUSIONS

The discoidal complex studied here is a useful system for molecular dynamics studies of lipid/protein complexes. Sampling of the peptide structure and dynamics benefits from the fact that there are several copies of the 18A peptide. This aids in the study of local structure, such as particular interhelix salt bridges, but does not help in the sampling of global or collective structure and dynamics.

Interhelix energetics were found to be dominated by salt bridges. Salt bridging provides a means of creating specificity in interhelix interactions. Solvated side chains can form salt-bridged conformations, as seen from the examples of salt-bridge formation observed. The side chains involved can fluctuate between salt-bridged and non-salt-bridged conformations and still contribute substantially to the average interhelical energy. Based on this simulation, salt bridging is expected to be the primary determinant of the arrangement of helices relative to each other in lipoproteins. Whereas this may be limited primarily to determining a parallel or antiparallel orientation of helices in a picket fence model disc, for rail fence models salt bridging is expected to determine helix registry. Because Apo A-I discs, such as natural nascent HDL, are likely to contain the rail fence orientation (Borhani et al., 1997), the importance of salt bridging suggested by this simulation is of general significance. Salt bridges are expected to be particularly important in lipoproteins because the hydrophobic sides of the α-helices face lipid, and so hydrophobic interactions between helices are difficult to form and are relatively nonspecific. Based on our results we expect interhelix salt bridging to be one reason, perhaps the major reason, for the existence of the characteristic class A charge distribution.

TABLE 1 Number of salt bridge formations and disruptions for significant salt bridges (all helices and all time steps)

Salt bridge	Total formations	Total disruptions
Odd* D8-K15	5	5
Even[#] K9-E12	1	0
Intra[§] K4-D8	1	0
Intra K9-E12	2	3
Intra K13-E16	2	5

*Odd: Interhelix, odd interface.
[#]Even: Interhelix, even interface.
[§]Intra: Intrahelix.

We thank the Theoretical Biophysics Group of the Beckman Institute for Advanced Science and Technology at the University of Illinois Urbana-Champaign for generous allocations of computer time and for valued help with NAMD and VMD.

This work was supported by grants PO1 HL 34343 (J. P. Segrest, PI) and P41 RR05969 (K. Schulten, PI) from the National Institutes of Health and by National Science Foundation (grant BIR 94–23827) (K. Schulten, PI). We are indebted to Jere Segrest, G. M. Anantharamiah, Vinod Mishra, David Borhani, Christie Brouillette, and Klaus Schulten for stimulating discussions.

REFERENCES

Alper, H. E., and T. R. Stouch. 1995. Orientation and diffusion of a drug analogue in biomembranes: molecular dynamics simulations. *J. Phys. Chem.* 99:5724–5731.

Anantharamaiah, G. M., J. L. Jones, C. G. Brouillette, C. F. Schmidt, B. H. Chung, T. A. Hughes, A. S. Brown, and J. P. Segrest. 1985. Studies of synthetic peptide analogs of the amphipathic helix: structure of complexes with dimyristoyl phosphatidylcholine. *J. Biol. Chem.* 260: 10248–10255.

Anderson, D. E., W. J. Becktel, and F. W. Dahlquist. 1990. pH-induced denaturation of proteins: a simple salt bridge contributes 3–5 kcal/mol to the free energy of folding of T4 lysozyme. *Biochemistry.* 29:2403–2408.

Atkinson, D., D. M. Small, and G. G. Shipley. 1980. X-ray and neutron scattering studies of plasma lipoproteins. *Ann. N.Y. Acad. Sci.* 348: 284–296.

Atkinson, D., H. M. Smith, J. Dickson, and J. P. Austin. 1976. Interaction of apoprotein from porcine high-density lipoprotein with dimyristoyl lecithin. 1. The structure of the complexes. *Eur. J. Biochem.* 64: 541–547.

Bassolino-Klimas, D., H. E. Alper, and T. R. Stouch. 1995. Mechanism of solute diffusion through lipid bilayer membranes by molecular dynamics simulation. *J. Am. Chem. Soc.* 117:4118–4129.

Borhani, D. W., D. P. Rogers, J. A. Engler, and C. G. Brouillette. 1997. Crystal structure of truncated human apolipoprotein A-I suggests a lipid bound conformation. *Proc. Natl. Acad. Sci. USA.* 94:12291–12296.

Bradley, E. K., J. F. Thomason, F. E. Cohen, P. A. Kosen, and I. D. Kuntz. 1990. Studies of synthetic helical peptides using circular dichroism and nuclear magnetic resonance. *J. Mol. Biol.* 215:607–622.

Brasseur, R., J. DeMutter, B. VanLoo, E. Goormaghtigh, J. M. Ruysschaert, and M. Rosseneu. 1990. Mode of assembly of amphipathic helical segments in model high-density lipoproteins. *Biochim. Biophys. Acta.* 1043:245–252.

Breiter, D. R., M. R. Kanost, M. M. Benning, G. Wesenberg, J. H. Law, M. A. Wells, I. Rayment, and H. M. Holden. 1991. Molecular structure of an apolipoprotein determined at 2.5 Å resolution. *Biochemistry.* 30:603–608.

Brooks, B. R., R. E. Bruccoleri, B. D. Olafson, D. J. States, S. Swaminathan, and M. Karplus. 1983. CHARMM: a program for macromolecular energy, minimization and dynamics calculations. *J. Comp. Chem.* 4:187–217.

Brouillette, C. G., and G. M. Anantharamaiah. 1995. Structural models of human apolipoprotein A-I. *Biochim. Biophys. Acta.* 1256:103–129.

Brünger, A. 1992. X-PLOR, Version 3.1: A System for X-Ray Crystallography and NMR. Yale University Press, New Haven, CT.

Carson, M. 1991. Ribbons 2.0. *J. Appl. Crystallogr.* 24:958–961.

Chiu, S. W., M. Clark, V. Balaji, S. Subramaniam, H. L. Scott, and E. Jakobsson. 1995. Incorporation of surface tension into molecular dynamics simulation of an interface: a fluid phase lipid bilayer membrane. *Biophys. J.* 69:1230–1245.

Chung, B. H., G. M. Anantharamaiah, C. G. Brouillette, T. Nishida, and J. P. Segrest. 1985. Studies of synthetic peptide analogs of the amphipathic helix: correlation of structure with function. *J. Biol. Chem.* 260:10256–10262.

Corijn, J., R. Deleys, C. Labeur, B. Vanloo, L. Lins, R. Brasseur, J. Baert, J. M. Ruysschaert, and M. Rosseneu. 1993. Synthetic model peptides for apolipoproteins. II. Characterization of the discoidal complexes generated between phospholipids and synthetic model peptides for apolipoproteins. *Biochim. Biophys. Acta.* 1170:8–16.

Damodaran, K. V., and K. M. Merz. 1994. A comparison of DMPC- and DLPE-based lipid bilayers. *Biophys. J.* 66:1076–1087.

Damodaran, K. V., and K. M. Merz. 1995. Interaction of the fusion inhibiting peptide carbobenzoxy-D-Phe-L-Phe-Gly with *N*-methyldioleoylphosphatidylethanolamine lipid bilayers. *J. Am. Chem. Soc.* 117: 6561–6571.

Damodaran, K. V., K. M. Merz, and B. P. Gaber. 1992. Structure and dynamics of the dilaurylphosphatidylethanolamine lipid bilayer. *Biochemistry.* 31:7656–7664.

Damodaran, K. V., K. M. Merz, and B. P. Gaber. 1995. Interaction of small peptides with lipid bilayers. *Biophys. J.* 69:1299–1308.

De Loof, H., S. C. Harvey, J. P. Segrest, and R. W. Pastor. 1991. Mean field stochatic boundary molecular dynamics simulation of a phospholipid in a membrane. *Biochemistry.* 30:2099–2113.

Edholm, O., O. Berger, and F. Jahnig. 1995. Structure and fluctuations of bacteriorhodopsin in the purple membrane. *J. Mol. Biol.* 250:94–111.

Edholm, O., and A. M. Nyberg. 1992. Cholesterol in model membranes: a molecular dynamics simulation. *Biophys. J.* 63:1081–1089.

Epand, R. M., W. K. Surewicz, D. W. Hughes, H. Mantsch, J. P. Segrest, T. M. Allen, and G. M. Anantharamaiah. 1989. Properties of lipid complexes with amphipathic helix-forming peptides: role of distribution of peptide charges. *J. Biol. Chem.* 264:

Feller, S. E., D. Yin, R. W. Pastor, and A. D. MacKerell. 1997. Molecular dynamics simulation of unsaturated lipid bilayers at low hydration: parameterization and comparison with diffraction studies. *Biophys. J.* 73:2269–2279.

Heller, H., M. Schaefer, and K. Schulten. 1993. Molecular dynamics of a bilayer of 200 lipids in the gel and in the liquid-crystal phases. *J. Phys. Chem.* 97:8343–8360.

Hendsch, Z. S., and B. Tidor. 1994. Do salt bridges stabilize proteins? A continuum electrostatic analysis. *Protein Sci.* 3:211–226.

Huang, P., and G. H. Loew. 1995. Interaction of an amphiphilic peptide with a phospholipid bilayer surface by molecular dynamics simulation study. *J. Biomol. Struct. Dyn.* 12:937–956.

Huang, P., J. J. Perez, and G. H. Loew. 1994. Molecular dynamics simulations of phospholipid bilayers. *J. Biomol. Struct. Dyn.* 11: 927–956.

Humphrey, W., A. Dalke, and K. Schulten. 1996. VMD—visual molecular dynamics. *J. Mol. Graph.* 14:33–38.

Huyghues-Despointes, B. M. P., and R. L. Baldwin. 1997. Ion-pair and hydrogen bond interactions between histidine and aspartate in a peptide helix. *Biochemistry.* 36:1965–1970.

Jones, M. K., G. M. Anantharamaiah, and J. P. Segrest. 1992. Computer programs to identify and classify amphipathic alpha helical domains. *J. Lipid Res.* 33:287–296.

Jorgensen, W. L., J. Chandrasekhar, and J. D. Madura. 1983. Comparison of simple potential functions for simulating liquid water. *J. Chem. Phys.* 79:926–935.

Loncharich, R. J., Brooks, B. R., and Pastor, R. W. 1992. Langevin dynamics of peptides: the frictional dependence of isomerizatin rates of N-acetylalanyl-N-′-methylamide. *Biopolymers*. 32:523–535.

Lumb, K. J., and P. S. Kim. 1995. Measurement of the interhelical electrostatic interactions in the CGN4 leucine zipper. *Science.* 268: 436–439.

Lund-Katz, S., M. C. Philips, V. K. Mishra, J. P. Segrest, and G. M. Anantharamaiah. 1995. Microenvironments of basic amino acids in amphipathic alpha-helices bound to phospholipid: ^{13}C NMR studies using selectively labeled peptides. *Biochemistry*. 34:9219–9226.

Lyu, P. C., P. J. Gans, and N. R. Kallenbach. 1992. Energetic contribution of solvent-exposed ion pairs to alpha-helix structure. *J. Mol. Biol.* 223:343–350.

MacKerell, A. D., Jr., D. Bashford, M. Bellot, R. L. Dunbrack, Jr., J. Evanseck, M. J. Field, S. Fischer, J. Gao, H. Guo, S. Ha, D. Joseph, L. Kuchnir, K. Kuczera, F. T. K. Lau, C. Mattos, S. Michnick, T. Ngo, D. T. Nguyen, B. Prodhom, W. E. Reiher, III, B. Roux, M. Schlenkrich, J. Smith, R. Stote, J. Straub, M. Watanabe, J. Wiorkiewicz-Kuczera, D. Yin, and M. Karplus. 1998. All-atom empirical potential for molecular modeling and dynamics studies of proteins. *J. Phys. Chem. B.* 102: 3586–3616.

Marqusee, S., and R. L. Baldwin. 1987. Helix stabilization by $Glu^{-}..Lys^{+}$ salt bridges in short peptides of de novo design. *Proc. Natl. Acad. Sci. USA.* 84:8898–8902.

Mishra, V. K., M. N. Palgunachari, J. P. Segrest, and G. M. Anantharamaiah. 1994. Interactions of synthetic peptide analogs of the class A amphipathic helix with lipids: interactions with lipids. *J. Biol. Chem.* 269:7185–7191.

Nakamura, H. 1996. Roles of electrostatic interactions in proteins. *Q. Rev. Biophys.* 29:1–90.

Nelson, M., W. Humphrey, A. Gursoy, A. Dalke, L. Kale, R. D. Skeel, and

K. Schulten. 1996. NAMD—a parallel, object-oriented molecular dynamics program. *J. Supercomput. Appl.* 10:251–268.

Pastor, R. W. 1994. Molecular dynamics and Monte Carlo simulations of lipid bilayers. *Curr. Opin. Struct. Biol.* 4:486–492.

Pearce, L. L., and S. C. Harvey. 1993. Langevin dynamics studies of unsaturated phospholipids in a membrane environment. *Biophys. J.* 65:1084–1092.

Phillips, J. C., W. Wriggers, Z. Li, A. Jonas, and K. Schulten. 1997. Predicting the structure of apolipoprotein A-I in reconstituted lipoprotein disks. *Biophys. J.* 73:2337–2346.

Raussens, V., V. Narayanaswami, E. Goormaghtigh, R. O. Ryan, and J. M. Ruysschaert. 1995. Alignment of the apolipophorin III alpha helices in complexes with dimyristoylphosphatidylcholine: a unique spatial orientation. *J. Biol. Chem.* 270:12542–12547.

Schlenkrich, M., J. Brickmann, A. D. MacKerell, Jr., M. Karplus. 1996. Empirical potential energy function for phospholipids: criteria for parameter optimization and applications. *In* Biological Membranes: A Molecular Perspective from Computation and Experiment. K. M. Merz and B. Roux, editors. Birkhäuser, Boston. 31–81.

Segrest, J. P. 1977. Amphipathic helixes and plasma lipoproteins: thermodynamic and geometric considerations. *Chem. Phy. Lipids.* 18:7–22.

Segrest, J. P., D. W. Garber, C. G. Brouillette, S. C. Harvey, and G. M. Anantharamaiah. 1994. The amphipathic alpha helix: s multifunctional structural motif in plasma apolipoproteins. *Adv. Protein Chem.* 45: 303–369.

Smith, J. S., and J. M. Scholtz. 1998. Energetics of polar side-chain interactions in helical peptides: salt effects on ion pairs and hydrogen bonds. *Biochemistry.* 37:33–40.

Tall, R., D. M. Small, R. J. Deckelbaum, and G. G. Shipley. 1977. Structure and thermodynamic properties of high density lipoprotein recombinants. *J. Biol. Chem.* 252:4701–4711.

Tu, K., D. J. Tobias, and M. L. Klein. 1995. Constant pressure and temperature molecular dynamics simulation of a fully hydrated liquid crystal phase dipalmitoylphosphatidylcholine bilayer. *Biophys. J.* 69: 2558–2562.

Wald, J. H., E. Goormaghtigh, J. DeMutter, J. M. Ruysschauer, and A. Jonas. 1990. Investigation of the lipid domains and apolipoprotein orientation in reconstituted high density lipoproteins by fluororescence and IR methods. *J. Biol. Chem.* 265:20044–20055.

Wiener, M. C., and S. H. White. 1992. Structure of a fluid dioleoylphosphatidylcholine bilayer determined by joint refinement of x-ray and neutron diffraction data. III. Complete structure. *Biophys. J.* 61: 434–447.

Wilson, C., M. R. Wardell, K. H. Weisgraber, R. W. Mahley, and D. A. Agard. 1991. Three-dimensional structure of the LDL receptor-binding doman of human apolipoprotein E. *Science.* 252:1817–1822.

Woolf, T. B., and B. Roux. 1996. Structure, energetics, and dynamics of lipid-protein interactions: a molecular dynamics study of the gramicidin A channel in a DMPC bilayer. *Proteins.* 24:92–114.

Zhou, F., and K. Schulten. 1995. Molecular dynamics study of a membrane-water interface. *J. Phys. Chem.* 99:2194–2207.